

DMSS: A Robust Deep Meta Structure Based Similarity Measure in Heterogeneous Information Networks

Yu Zhou · Jianbin Huang · Heli Sun ·
Yizhou Sun · Hong Cheng

Received: date / Accepted: date

Abstract Similarity measure as a fundamental task in heterogeneous information network analysis has been applied to many areas, e.g. product recommendation, clustering and web search. The state-of-the-art metrics depend on meta paths or meta structures specified by users. In this paper, a novel similarity measure on heterogeneous information networks, called Deep Meta Structure based Similarity (*DMSS*), is proposed. The deep meta structure as a schematic structure on heterogeneous information networks provides a unified framework integrating all the meta paths and meta structures. It can be constructed automatically. In order to formalize the semantics encapsulated in the deep meta structure, we decompose it into several deep meta paths, and then combine all the commuting matrices of these deep meta paths according to different weights. It is noteworthy that the weights can be determined by the proposed strategy. As a result, *DMSS* is defined by virtue of the final commuting matrix and therefore is robust to different schematic structures. Experimental evaluations show that the state-of-the-art metrics are really sensitive to meta paths or meta structures in terms of clustering and ranking.

Yu Zhou
School of Software, Xidian University, Xi'an, China.
E-mail: peterjone85@hotmail.com

Jianbin Huang
School of Software, Xidian University, Xi'an, China.
E-mail: jbh Huang@xidian.edu.cn

Heli Sun
Department of Computer Science and Technology, Xi'an Jiaotong University, Xi'an, China.
E-mail: hlsun@mail.xjtu.edu.cn

Yizhou Sun
Department of Computer Science, UCLA, Los Angeles, USA.
E-mail: yzsun@cs.ucla.edu

Hong Cheng
Systems Engineering and Engineering Management, CUHK, Hong Kong, China.
E-mail: hcheng@se.cuhk.edu.hk

Besides, *DMSS* outperforms the state-of-the-art metrics in terms of ranking and clustering in the case of selecting an appropriate decaying parameter.

Keywords Heterogeneous Information Network · Similarity · Deep Meta Path · Meta Path · Meta Structure

1 Introduction

As well known, information networks can be used to model many real systems such as biological system and social media. As a result, information network analysis becomes a hot research topic in the field of graph mining. Many researchers are concerned with information networks with single-typed components, the kind of which is called homogeneous information network. However, the real information networks usually consist of interconnected and multi-typed components. This kind of information networks are generally called **Heterogeneous Information Networks (HIN)**. Mining heterogeneous information networks attracts many researchers' attentions.

Fig. 1 shows a toy bibliographic information network with four actual object types, i.e. *Author* (*A*), *Paper* (*P*), *Venue* (*V*) and *Term* (*T*). The type *Author* contains four instances: Yizhou Sun, Jiaswei Han, Philip S. Yu, and Jie Tang. The type *Venue* contains four instances: VLDB, AAAI, KDD, TKDE. The type *Paper* contains six instances: PathSim [9], GenClus [18], RAIN [29], TPFPG [30], SpiderMine [31] and HeteSim [13]. The type *Term* contains six instances: Pattern, Information, Mining, Social, Clustering, Similarity and Network. Each paper published at a venue must have its author(s) and its related terms. Hence, they contain three types of links: $P \leftrightarrow A$, $P \leftrightarrow V$ and $P \leftrightarrow T$.

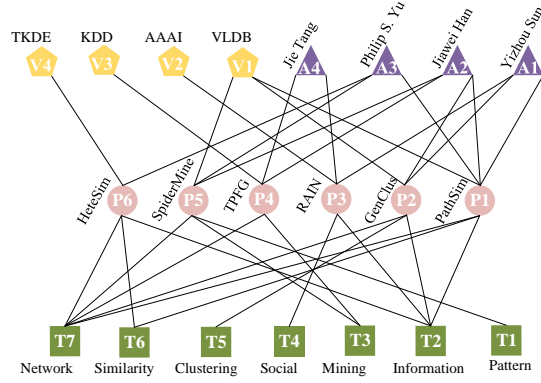


Fig. 1 A Toy Bibliographic Information Network with actual papers, authors, terms and venues. The triangles, circles, squares, and pentagons respectively stand for authors, papers, terms and venues.

Given a **HIN** G , a fundamental problem is to measure the similarity $s(o_s, o_t)$ of two objects o_s and o_t . The state-of-the-art metrics depend on user-

specified schematic structures. For example, *PathSim* [9] and Biased Path Constrained Random Walk (*BPCRW*) [15,14] take a meta path specified by users as an input, and Biased Structure Constrained Subgraph Expansion (*BSCSE*) [20] takes a meta structure specified by users as an input. This causes a terrible problem that these metrics are strongly sensitive to pre-specified schematic structures. That means the users must know how to select an appropriate schematic structure. Obviously, this is difficult for users. For example, a biological information networks contain many object types, e.g. Gene, Gene Ontology, Tissue, Chemical Compound, Side Effect, Substructure, Chemical Ontology, Pathway, Disease, Gene Family etc. [22,23]. It is impossible for users to know which schematic structures is appropriate. Moreover, the literature [20] thought that meta paths can only capture biased and relatively simple semantics. Therefore, its authors proposed the meta structure in order to capture more complex semantics. In fact, the meta structure can only capture biased semantics. The biases will be shown in section 3.2. The meta paths and meta structures are collectively referred to as schematic structures in this paper.

To overcome the above limitations, we aim to devise an automatically-constructed schematic structure not depending on any pre-specified meta paths or meta structures. A feasible way is to construct a schematic structure combining all the meta paths or meta structures by traversing the network schema. Obviously, this ensures the schematic structure does not depend on any pre-specified meta paths or meta structures. Subtree pattern (also called tree-walks) proposed in [28] is a quasi spanning tree in graphs. The difference from the traditional spanning tree is that nodes can be re-visited in the process of traversing the graphs. The idea of constructing the subtree pattern can be employed here. In this paper, we devise a hierarchical schematic structure called Deep Meta Structure (**DeepMS**) consisting of the object types with different layer labels. It can be automatically constructed via repetitively visiting the object types on the network schema. Note in particular that the **DeepMS** contains all the meta paths and meta structures.

After obtaining the **DeepMS**, we should extract semantics encapsulated in it. However, this is difficult because the **DeepMS** is complicated and the objects types are coupled tightly. To decouple the object types, it can be decomposed into several deep meta paths. Then, we define the commuting matrices of the deep meta paths as similarly as those of meta paths. As a result, *DMSS* is defined as the weighted summation of all the commuting matrices of the deep meta paths. Obviously, the proposed *DMSS* is robust to different schematic structures, i.e. meta paths or meta structures, because it considers all the possible structures. We propose a strategy to automatically determine the weights of different deep meta paths. This strategy is based on the roles of different meta paths in the **HINs**.

The main contributions are summarized as follows.

- 1) We propose the deep meta structure, which contains all the meta paths and meta structures. It can be constructed automatically. In order to decouple

the object types, the deep meta structure is decomposed into several deep meta paths;

- 2) We define the commuting matrices of the deep meta paths, and propose a strategy to determine the weights of different deep meta paths. The proposed *DMSS* is defined as the weighted summation of all these commuting matrices. It is noteworthy that *DMSS* is robust to schematic structures.
- 3) We conduct experiments for evaluating the performance of the proposed metric *DMSS*; *DMSS* outperforms the baselines in terms of ranking quality and clustering quality in the case of selecting an appropriate decaying parameter. In addition, we discover that the state-of-the-art metrics are really sensitive to different schematic structures. This also reflects the advantage of *DMSS*.

The rest of the paper is organized as follows. Section 2 introduces related works. Section 3 provides some preliminaries on **HINs**. In section 4, we define the commuting matrix of a meta structure, and employ it to re-define *BSCSE*. Section 5 introduces the definition of *DMSS*. The experimental evaluations are introduced in section 6. The conclusion is introduced in section 7.

2 Related Work

In this section, we summarize the works related to the **HIN**. To the best of our knowledge, Sun et al. [1] first proposed the bi-type information network, and integrated clustering and ranking for analyzing it. In the article [2], She extended the bi-type information network to the heterogeneous information network with star network schema and studied ranking-based clustering on it. The literatures [3,4] gives a comprehensive summarization of research topics on **HINs** including similarity measure, clustering, classification, link prediction, ranking, recommendation, information fusion and other applications. Below, we only summarize the works on similarity measures on information networks.

Homogeneous Information Network. At the beginning, similarity measures are studied on homogeneous information networks. These studies include feature-based similarity measures and link-based similarity measures [4]. Feature based similarity measures include cosine similarity, Jaccard coefficient, Euclidean distance and Minkowski distance [5]. However, the feature based similarity measures ignore the link information on homogeneous information networks. The link based similarity measures [6,7] address this issues. Article [6] proposed a general similarity measure *SimRank*, which thought two similar objects must relate to similar objects, combining the link information. Article [7] evaluated the similarities of objects by a random walk model with restart. In article [8], the authors summarize the off-the-shelf works on the link prediction including many state-of-the-art similarity measures in homogeneous information networks.

Heterogeneous Information Network. Recently, many researchers focus on the similarity measure on **HINs**. **HINs** contain rich semantic information in addition to the structural information. This is completely different from

homogeneous information networks. Therefore, similarity measures on **HINs** must integrate these two kinds of information together. Sun [9] first proposed a meta path based similarity measures, called *PathSim*, on **HINs**. Xiong et al. [12] studied the problem of obtaining the top- k similar object pairs based on user-specified join paths. Shi et al. [13] extended the similarity measure on **HINs** to the relevance measure which can be used to evaluate the relatedness of two object with different types. For an user-specified meta path, His method *HeteSim* is based on the pairwise random walk from its two endpoints to its center. Lao and Cohen [14,15] proposed a Path Constrained Random Walk (**PCRW**) model to evaluate the entity similarity in labeled directed graphs. This model can be applied to measuring the similarity of objects on **HINs**. Usman et al. extend *SimRank* to the heterogeneous information networks using the tensor techniques. Article [11] proposed a socialized word embedding algorithm integrating user’s personal characteristics and user’s social relationship on social media.

3 Preliminaries

In this section, we introduce the definition of **HINs** and some important concepts related to it, e.g. network schema in section 3.1, meta paths and meta structures in section 3.2. the network schema of a **HIN** is essentially its template guiding the generation of the **HIN**. The meta paths and meta structures are two kinds of semantic structure. They can capture semantics encapsulated in the **HINs**.

3.1 The HIN Model.

An information network [17] is a directed graph $G = (V, E, \mathcal{A}, \mathcal{R})$ where V is a set of objects and E is a set of links. \mathcal{A} and \mathcal{R} respectively denote the set of object types and link types. For any object $v \in V$, it belongs to an object type $\phi(v) \in \mathcal{A}$. For any link $e \in E$, it belongs to a link type $\psi(e) \in \mathcal{R}$. In essence, $\psi(e)$ represents a relation from its source object type to its target object type. If two links belong to the same link type, they share the same starting object type as well as the ending object type. G is called a **Heterogeneous Information Network** if $|\mathcal{A}| > 1$ or $|\mathcal{R}| > 1$. Otherwise, it is called a homogeneous information network.

The **HIN** G consists of multi-typed objects and links. It can essentially be formed according to a template called its network schema. In general, the **Network schema** $\Theta_G = (\mathcal{A}, \mathcal{R})$ [17] of G is a directed graph consisting of the object types in \mathcal{A} and the link types in \mathcal{R} . Link types in G are essentially the relations from source object types to target object types. Fig. 2(a) shows the network schema for the **HIN** in Fig. 1. Many biological networks can be modeled as **HINs** as well. In this paper, we use a biological information network with six object types *Gene* (G), *Tissue* (T), *GeneOntology* (GO), *Chemical-Compound* (CC), *Substructure* (Sub) and *SideEffect* (Si) as an example. It

contains five link types $GO \leftrightarrow G$, $T \leftrightarrow G$, $G \leftrightarrow CC$, $CC \leftrightarrow Si$, $CC \leftrightarrow Sub$. Its network schema is shown in 2(b).

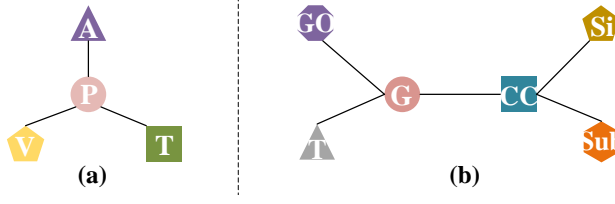


Fig. 2 (a) Bibliographic network schema. (b) Biological network schema.

3.2 Meta Paths and Meta Structures.

There are rich semantics in **HIN** G . These semantics can be captured by paths or more complicated structures in Θ_G . We below introduce two kinds of semantic structures, i.e. meta paths and meta structures.

The meta path [9], denoted by $C_1 \xrightarrow{R_1} C_2 \xrightarrow{R_2} \dots \xrightarrow{R_{l-2}} C_{l-1} \xrightarrow{R_{l-1}} C_l$, $C_i \in \mathcal{A}, i = 1, \dots, l$ and $R_j \in \mathcal{R}, j = 1, \dots, l-1$, is an alternate sequence of object types and link types. Note that R_j is a link type starting from C_j to $C_{j+1}, j = 1, \dots, l-1$. In essence, R_j is a relation from C_j to C_{j+1} . The meta path is essentially a composite relation $R_1 \circ R_2 \circ \dots \circ R_{l-1}$. That implies it can capture semantic information contained in the network schema.

In practice, the meta path $\mathcal{P} = C_1 \xrightarrow{R_1} C_2 \xrightarrow{R_2} \dots \xrightarrow{R_{l-2}} C_{l-1} \xrightarrow{R_{l-1}} C_l$ can be compactly denoted as $(C_1, C_2, \dots, C_{l-1}, C_l)$ unless stated otherwise. There are some useful concepts related to \mathcal{P} : (1) **length** of \mathcal{P} , (2) **path instance** following \mathcal{P} , (3) **reverse meta path** of \mathcal{P} , (4) **symmetric meta path**, (5) **commuting matrix** $\mathcal{M}_{\mathcal{P}}$ of \mathcal{P} , see literature [9].

Different meta paths carry different semantics. (A, P, A) shown in Fig. 3(a) carry the information “Two authors cooperate on a paper”. However, literature [20] pointed out meta paths can only capture relatively simple and biased semantics. For example, (A, P, V, P, A) captures “Two authors write a paper published on the same venue”, but neglects “Two authors write a paper containing the same term”. To overcome this issue, [20] proposed the meta structure.

Formally, a **meta structure** $\mathcal{S} = (\mathcal{V}_{\mathcal{S}}, \mathcal{E}_{\mathcal{S}}, T_s, T_t)$ is a directed acyclic graph with a single source object type T_s and a single target object type T_t . $\mathcal{V}_{\mathcal{S}}$ is a set of object types, and $\mathcal{E}_{\mathcal{S}}$ is a set of link types. For ease of presentation, the meta structures shown in Fig. 3(b,c,d) can be respectively denoted as $(A, P, (V, T), P, A)$, $(G, (GO, T), G)$ and $(V, P, (A, T), P, V)$. Different meta structures carry different semantics. The meta structure shown in Fig. 3(b) expresses the information “Two authors write a paper both published on the same venue and containing the same term”, but ignores the information “Two

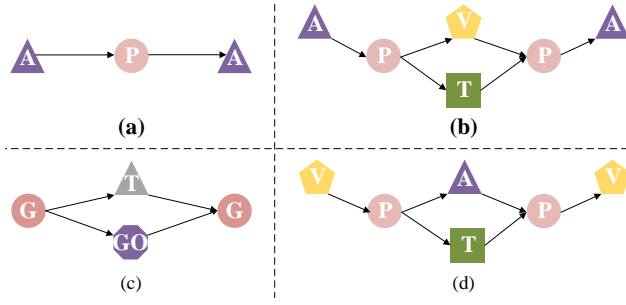


Fig. 3 Some Meta Paths and meta structures on the network schema shown in Fig. 2(a,b).

authors cooperate on a paper.” That means the meta structure carries biased semantics.

More importantly, both meta paths and meta structures need to be specified by users. On the **HINs** like the bibliographical information networks, it may be relatively easy for users to specify meta paths or meta structures. However, specifying meta paths or meta structures becomes very difficult on the **HINs** like the biological information networks, because in reality it contains many object types (Gene, Gene Ontology, Tissue, Chemical Compound, Chemical Ontology, Side Effect, Substructure, Pathway, Disease and Gene Family) and many relations. In Fig. 2(b), we give a biological network schema only containing six object types and five link types.

In this paper, we aim to define a similarity measure on **HINs**, which does not depend on any meta paths or meta structures. Formally, the problem takes a **HIN**, a source object as input, and then outputs a vector whose entries denote the similarity between the source object to the target object. Below, we first use commuting matrices to re-define the meta structure based similarity (*BSCSE*).

4 Commuting Matrices of Meta Structures

Given a meta structure \mathcal{S} , we sort its object types with regard to the topological order. Suppose its height is equal to h_1 . Similarly, let L_i denote the set of object types on the layer i , C_{L_i} denote the cartesian product of the set of objects belonging to different types in L_i , $i = 0, 1, \dots, h_1 - 1$. The relation matrix $W_{L_i L_{i+1}}$ from C_{L_i} to $C_{L_{i+1}}$ is defined as the one whose entries (s, t) are equal to 1 if the s -th element $C_{L_i}(s)$ of C_{L_i} is adjacent to the t -th one $C_{L_{i+1}}(t)$ of $C_{L_{i+1}}$ in G , otherwise 0. $C_{L_i}(s)$ and $C_{L_{i+1}}(t)$ are adjacent if and only if for any $u \in C_{L_i}(s)$ and $v \in C_{L_{i+1}}(t)$, u and v are adjacent on the **HIN** G . The commuting matrix of the meta structure is defined as $\mathcal{M}_{\mathcal{S}} = \prod_{i=0}^{h_1-1} W_{L_i L_{i+1}}$. Each entry in $\mathcal{M}_{\mathcal{S}}$ also represents the number of instances following \mathcal{S} . The commuting matrix of its reverse is equal to $\mathcal{M}_{\mathcal{S}}^T$.

For a given meta structure, its *BSCSE* with $\alpha = 1$ can be expressed by its commuting matrix as well. The following lemma 1 describes this conclusion.

Throughout this paper, we use $\bar{X} = U_X^{-1}X$ to denote its normalized version, where U_X is a diagonal matrix whose nonzero entries are equal to the row sum of X .

Lemma 1 *Given a meta structure \mathcal{S} , suppose that L_i denotes the set of object types on its i -th layer. When $\alpha = 1$,*

$$BSCSE(o_s, o_t | \mathcal{S}, h, \alpha) = \mathcal{M}_{\mathcal{S}}^h(o_s, o_t),$$

where $\mathcal{M}_{\mathcal{S}}^h = \bar{W}_{L_0 L_1} \times \bar{W}_{L_1 L_2} \times \cdots \times \bar{W}_{L_{h-1} L_h}$.

Proof We prove the lemma by induction on $h \geq 1$.

Initial Step. Obviously, $C_{L_0} = \{o_s\}$. When $h = 1$, $\mathcal{M}_{\mathcal{S}}^1 = \bar{W}_{L_0 L_1}$. Assume there are d_s different object tuples in C_{L_1} adjacent to o_s , denoted as $o_{11}, o_{12}, \dots, o_{1d_s}$. According to the definition of $w(v)$ [20], $w(o_{1i}) = \frac{1}{d_s}, i = 1, 2, \dots, d_s$. Obviously, $\bar{W}_{L_0 L_1}(o_s, o_{1i}) = \frac{1}{d_s}, i = 1, 2, \dots, d_s$. Therefore, $BSCSE(o_s, o_{1i} | \mathcal{S}, 1, \alpha) = \mathcal{M}_{\mathcal{S}}^1(o_s, o_{1i}), i = 1, 2, \dots, d_s$.

Inductive Step. Assume the conclusion holds for h . Below, we prove it also holds for $h + 1$. Obviously,

$$\begin{aligned} \mathcal{M}_{\mathcal{S}}^{h+1} &= \mathcal{M}_{\mathcal{S}}^h \bar{W}_{L_h L_{h+1}} \\ &= \left[\sum_{k=1}^l x_k y_{k1}, \dots, \sum_{k=1}^l x_k y_{km} \right], \end{aligned} \quad (1)$$

where $\mathcal{M}_{\mathcal{S}}^h = [x_1, x_2, \dots, x_l]$, and $\bar{W}_{L_h L_{h+1}} = (y_{ij})_{l \times m}$. Note in particular that $x_i = BSCSE(o_s, o_i | \mathcal{S}, h, \alpha)$, where $i = 1, \dots, l$, and y_{ij} , where $i = 1, \dots, l, j = 1, \dots, m$, is equal to either 0 or $\frac{1}{|\{y_{ij} \neq 0 | j=1, \dots, m\}|}$. According to the definition of $BSCSE$ in literature [20],

$$BSCSE(o_s, o_j | \mathcal{S}, h+1, \alpha) = \sum_{k=1}^l x_k y_{kj}, j = 1, \dots, m. \quad (2)$$

Combining formulas 1 and 2, we have

$$BSCSE(o_s, o_j | \mathcal{S}, h+1, \alpha) = \mathcal{M}_{\mathcal{S}}^{h+1}(o_s, o_j),$$

where $j = 1, \dots, m$. The conclusion holds for $h + 1$.

5 DeepMS Based Similarity

This section is the main body of this paper. In section 5.1, we firstly present the architecture of the proposed deep meta structure. In section 5.2, we propose an approach to decomposing the deep meta structure into a collection of deep meta paths. Based on this decomposition, we define the proposed robust similarity measure $DMSS$ in section 5.3. In the last section, we describe the pseudo-code of the algorithm for computing $DMSS$ and analyze its time complexity.

5.1 Deep Meta Structure.

A **DeepMS** is essentially a hierarchical graph consisting of object types with different layer labels. It has two prominent advantages: (1) being automatically constructed by repetitively visiting object types in the process of traversing network schema; (2) combining all the meta paths and meta structures. Given a **HIN** G , we first extract its network schema Θ_G , and then select a source object type and a target object type. Unless stated otherwise, the source object type is the same as the target one. **The construction rule of the DeepMS \mathcal{D}_G of G** is described as follows. The source object type is placed on the 0-th layer. The object types on the layer $l = 1, 2, \dots, +\infty$ are composed of the neighbors of the object types on the layer $l-1$ on the network schema Θ_G . The adjacent object types are linked by an arrow pointing from the $(l-1)$ -th layer down to the l -th layer. Repeating the above process, we obtain the **DeepMS \mathcal{D}_G** . It is noteworthy that an object type may appear in adjacent layers of the **DeepMS** if there exist circles (or self-loops) in the network schema. At this time, one of them can be viewed as a copy of another one. Correspondingly, the objects belonging to this object type are also duplicated. Obviously, **DeepMS** contains all the meta paths and meta structures.

Fig. 5(a) shows the **DeepMS** of the network schema shown in Fig. 2(a). As shown in Fig. 4, it can be constructed as follows. A is both the source and target object type. Firstly, A is placed on the 0-th layer, see Fig. 4(a). P is placed on the 1-st layer, because P is the only neighbor of A in the network schema shown in Fig. 2(a), see Fig. 4(b). A , V and T are placed on the 3-rd layer, because they are the neighbors of P , see Fig. 4(c). Similarly, P is again placed on the 4-th layer, because it is the neighbor of A , V and T , see Fig. 4(d). At this time, P is visited again. Repeating the above procedure, we obtain the **DeepMS** shown in Fig. 5(a). Fig. 6(a) shows the **DeepMS** of the network schema shown in Fig. 2(b). Gene is both the source and target object type. It can be constructed as similarly as 5(a).

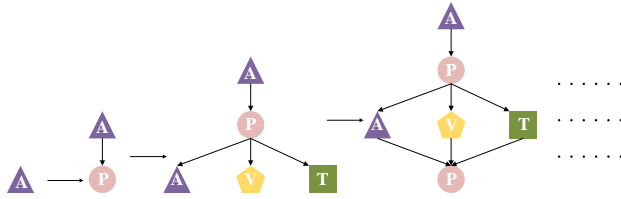


Fig. 4 Constructing the **DeepMS** of the toy bibliographic information network. The numbers near nodes stand for their layer labels

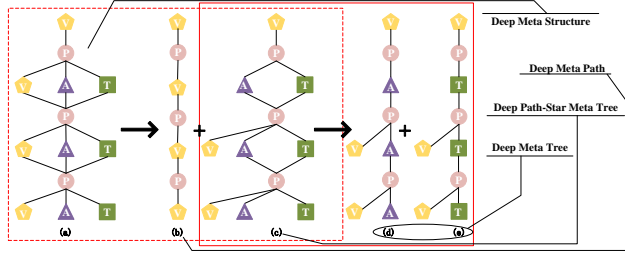


Fig. 5 Decomposing the **DeepMS** of the bibliographic network schema.

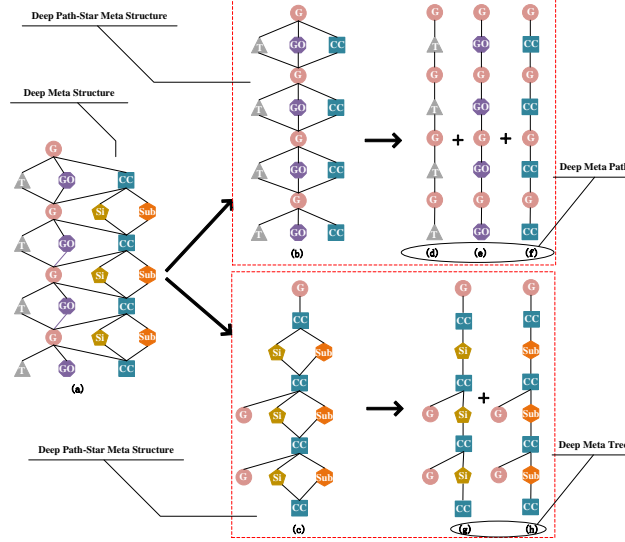


Fig. 6 Decomposing the **DeepMS** of the biological network schema.

5.2 Decomposition of DeepMS.

The object types with different layer labels are tightly coupled in the **DeepMS**. To decouple them, we should decompose the **DeepMS**. First of all, we introduce an augmented spanning tree of network schema, which is rooted at the source object type. If the network schema is a tree, its augmented spanning tree is equal to the network schema itself. If the network schema is not a tree, its augmented spanning tree is constructed based on its spanning tree as follows. The spanning tree of the network schema can be constructed using Breadth-First Search (BFS) starting from the source object type. Specifically, we traverse the spanning tree from top to bottom and from left to right. For the current object type in the process of traversing, if an edge adjacent to it in the network schema is not contained in the current spanning tree, we duplicate the object type adjacent to it and add an edge from it to the copied object type in the current spanning tree.

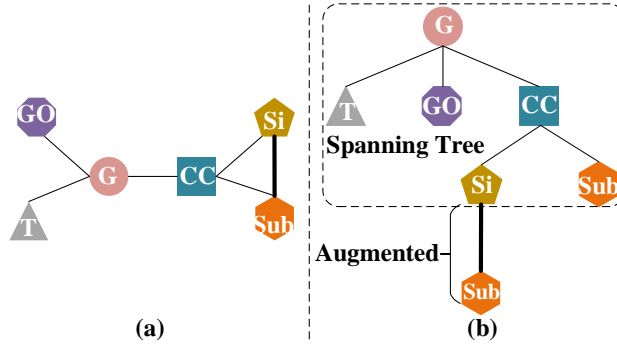


Fig. 7 Constructing the augmented spanning tree when the network schema is not a tree.

Now, we exemplify the construction of the augmented spanning tree when the network schema is not a tree. Suppose an edge (Si, Sub) is added to the network schema shown in Fig. 2(b). As a result, we get a new network schema shown in Fig. 7(a). Next, we show how to construct the augmented spanning tree for this network schema, see Fig. 7(b). Its spanning tree is enclosed by the dashed line frame. When we reach the node Si in the process of traversing, the edge (Si, Sub) incidental to Si is not contained in the spanning tree. So, we make a copy of the node Sub and add an edge from Si to the copied Sub .

After obtaining the augmented spanning tree, we traverse its internal nodes from top to bottom and from left to right. Each current object type is treated as a pivot, and therefore we obtain a subtree called path-star tree consisting of two parts: (1) the path from the root (i.e. the source object type) to the pivot; (2) the star consisting of the pivot as the center and its children. Then, we augment all these subtrees by repetitively duplicating the star substructure consisting of the pivotal object types and their children. For each copied pivotal object type, it is linked to the target object type by the path part of the path-star tree. Finally, we obtain several substructures of the **DeepMS**. In essence, the **DeepMS** can be viewed as the combination of these substructures. These substructures are called **deep path-star meta structures**. If the path-star tree is a single edge, the substructure generated by it is specially called **deep meta path**.

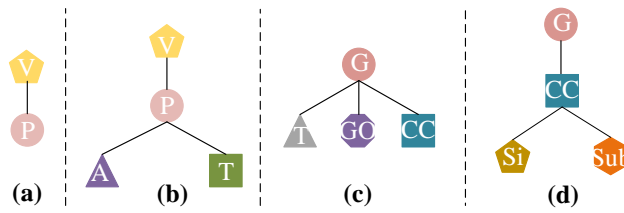


Fig. 8 Path-star trees of the bibliographic and biological network schema.

Here, we respectively take the bibliographic network schema and the biological network schema, shown in Fig. 2(a,b), as examples to present how to generate the path-star trees. For the bibliographic network schema, V is selected as the source object type. Its augmented spanning tree rooted at V is equal to the network schema itself because the bibliographic network schema is a tree. For the biological network schema, G is selected as the source object type. Its augmented spanning tree rooted at G is equal to the network schema itself because the biological network schema is a tree. After obtaining their augmented spanning trees, we traverse its internal nodes from top to bottom and from left to right. For the bibliographic network schema, its internal nodes are V and P . Its path-star trees are shown in Fig. 8(a,b). For the biological network schema, its internal nodes are G and CC . Its path-star trees are shown in Fig. 8(c,d).

Now, we augment the path-star tree of the bibliographic network schema. The object types V and P are respectively treated as the pivot. If V is the pivot, it has only one child P . Its path-star tree is a single edge, see Fig. 8(a). We repetitively duplicate its star part, and finally obtain a deep meta path shown in Fig. 5(b). It is noteworthy that the path part of the path-star tree is null at this time because the pivot V is the source object type. If P is the pivot, it has two children A and T . Its path-star tree is a tree, see Fig. 8(b). We repetitively duplicate its star part, and the pivot P is linked to the target object type V by the path part of the path-star tree. Finally, we obtain a deep path-star meta tree, see Fig. 5(c). Obviously, the **DeepMS** shown in Fig. 5(a) can be decomposed into the deep meta path (see Fig. 5(b)) and the deep path-star meta structure (see Fig. 5(c)).

Now, we augment the path-star tree of the biological network schema. The object types G and CC are respectively treated as the pivot. If G is the pivot, it has three children T , GO and CC . Its path-star tree is shown in Fig. 8(c). We repetitively duplicate its star part, and finally obtain a deep path-star meta structure shown in Fig. 6(b). At this time, the path part of the path-star tree is null because the pivot G is the source object type. If CC is the pivot, it has two children Si and Sub . Its path-star tree is shown in Fig. 8(d). We repetitively duplicate its star part, and the pivot CC is linked to each target object type G by the path part of the path-star tree. Finally, we obtain a deep path-star meta structure shown in Fig. 6(c). Obviously, the **DeepMS** shown in Fig. 6(a) can be decomposed into two deep path-star meta structures, respectively shown in Fig. 6(b,c).

After obtaining the deep path-star meta structures, we employ the commuting matrices of meta paths or the meta structures to extract semantics in them. For deep meta paths, it is relatively easy to do this. For deep path-star meta structures (not a path), the size of the commuting matrices may be very large because the cartesian product may yield a very large set. At this time, we still decompose the deep path-star meta structures into several simpler substructures called **deep meta trees**. The decomposition rule is to respectively consider each child of the pivotal object type. For example, the deep path-star meta structure shown in Fig. 5(c) can be decomposed into two

deep meta trees, see Fig. 5(d,e). The Fig. 5(d) only consider the object type A and the Fig 5(e) only consider the object type T . Similarly, the deep path-star meta structure shown in Fig. 6(b) is decomposed into three deep meta paths, see Fig. 6(d,e,f). The deep path-star meta structure shown in Fig. 6(c) is decomposed into two deep meta trees, see Fig. 6(g,h).

5.3 Similarity Measure.

In this section, we first define commuting matrices of deep meta paths, and then give a strategy to determine the weights of different meta paths.

For the deep meta path whose pivotal object type is the source object type \mathcal{T}_s , assume \mathcal{T}_c is one child of \mathcal{T}_s . The deep meta path \mathcal{D}_s can be briefly denoted as

$$\left(\mathcal{T}_s, \overbrace{\mathcal{T}_c, \mathcal{T}_s, \mathcal{T}_c}^{\text{repeated}}, \mathcal{T}_s, \dots \right). \quad (3)$$

Obviously, the substructure $(\mathcal{T}_c, \mathcal{T}_s, \mathcal{T}_c)$ recurrently appears in \mathcal{D}_s . Assume $W_{\mathcal{T}_s \mathcal{T}_c}$ denotes the relation matrix from \mathcal{T}_s to \mathcal{T}_c and $\bar{W}_{\mathcal{T}_s \mathcal{T}_c}$ is its normalized version. As a result, the commuting matrix of \mathcal{D}_s is defined as

$$\mathcal{M}_{\mathcal{D}_s} = \bar{W}_{\mathcal{T}_s \mathcal{T}_c} \times (\mathbf{I} - \lambda \bar{W}_{\mathcal{T}_s \mathcal{T}_c}^T \bar{W}_{\mathcal{T}_s \mathcal{T}_c})^{-1} \times \bar{W}_{\mathcal{T}_s \mathcal{T}_c}^T, \quad (4)$$

where $\lambda \in (0, 1)$ is called decaying parameter and \mathbf{I} is the identity matrix with the same size as $\bar{W}_{\mathcal{T}_s \mathcal{T}_c}^T \bar{W}_{\mathcal{T}_s \mathcal{T}_c}$. It is noteworthy that $\mathcal{M}_{\mathcal{D}_s}$ may be diagonal. At this time, \mathcal{D}_s is removed from all the deep meta paths because it can not provide any useful information for the similarities between source objects.

For the deep meta path whose pivotal object type \mathcal{T}_p is not the source object type \mathcal{T}_s , assume \mathcal{T}_c is one child of \mathcal{T}_p . Assume the deep meta path \mathcal{D}_p is compactly denoted as

$$\left(\mathcal{T}_s, \mathcal{T}_1, \dots, \mathcal{T}_n, \overbrace{\mathcal{T}_p, \mathcal{T}_c, \mathcal{T}_p}^{\text{repeated}}, \dots, \mathcal{T}_p, \mathcal{T}_n, \dots, \mathcal{T}_1, \mathcal{T}_s \right). \quad (5)$$

Obviously, the substructure $(\mathcal{T}_p, \mathcal{T}_c, \mathcal{T}_p)$ recurrently appears in \mathcal{D}_p . Therefore, the commuting matrix of \mathcal{D}_p is defined as

$$\mathcal{M}_{\mathcal{D}_p} = L \times \left(\mathbf{I} - \lambda \bar{W}_{\mathcal{T}_p \mathcal{T}_c} \bar{W}_{\mathcal{T}_p \mathcal{T}_c}^T \right)^{-1} \times L^T, \quad (6)$$

where

$$L = \bar{W}_{\mathcal{T}_s \mathcal{T}_1} \left(\prod_{i=1}^{n-1} \bar{W}_{\mathcal{T}_i \mathcal{T}_{i+1}} \right) \bar{W}_{\mathcal{T}_n \mathcal{T}_p}.$$

The deep meta paths only consider the structure of the network schema Θ_G , but ignore the structure of the **HIN** G . In fact, they have different importance in G because different deep meta paths have different numbers of path instances in G . Therefore, we should combine the commuting matrices of different deep meta paths according to different weights. Below, we introduce a strategy to determine these weights.

Take the deep meta path \mathcal{D}_p shown in the form 5 as an example. Assume \mathcal{T}_p is the current pivotal object type and the children of \mathcal{T}_p is $\mathcal{T}_{c_1}, \dots, \mathcal{T}_{c_m}$. We traverse the objects belonging to \mathcal{T}_p for N times, and then randomly sample an object from their neighbors. This sampled object must belong to $\mathcal{T}_{c_1}, \dots, \mathcal{T}_{c_{m-1}}$ or \mathcal{T}_{c_m} . Let $N_{\mathcal{T}_{c_i}}$ denote the number of the chosen objects belonging to \mathcal{T}_{c_i} . As a result, the weight between \mathcal{T}_p and \mathcal{T}_{c_i} is equal to $\omega_{\mathcal{T}_p \mathcal{T}_{c_i}} = \frac{N_{\mathcal{T}_{c_i}}}{N}$. For the deep meta path \mathcal{D}_p , its weight is equal to

$$\omega_{\mathcal{D}_p} = \omega_{\mathcal{T}_s \mathcal{T}_1} \left(\prod_{i=1}^{n-1} \omega_{\mathcal{T}_i \mathcal{T}_{i+1}} \right) \omega_{\mathcal{T}_n \mathcal{T}_p} \omega_{\mathcal{T}_p \mathcal{T}_c}. \quad (7)$$

In particular, if the user knows \mathcal{T}_{c_i} plays a more important role in determining the similarities of source objects than the other object types, then we can duplicate the objects belonging to \mathcal{T}_{c_i} to make sure that these objects are chosen in higher probability. For the bibliographic information network, A plays more important roles in determining the similarities of venues than T because authors are inclined to submitting their papers to the venues closely related to their research fields but terms may appear in the papers belonging to different research fields. At this time, we ceaselessly duplicate the objects belonging to A until the A object is picked in higher probability.

Now, we define the proposed similarity measure $DMSS$. Assume \mathcal{I} denote the set of internal object types in the augmented spanning tree. As a result,

$$DMSS(o_s, o_t) = \frac{\mathcal{U}(o_s, o_t)}{\mathcal{U}(o_s, o_s)}, \quad (8)$$

where

$$\mathcal{U} = \sum_{\mathcal{T}_p \in \mathcal{I}} \omega_{\mathcal{D}_p} \mathcal{M}_{\mathcal{D}_p}.$$

NOTE. According to formula 8, we only need to compute $\omega_{\mathcal{D}_p}$ and $\mathcal{M}_{\mathcal{D}_p}$ for each deep meta path. This means we can employ the distributed computing techniques to speed up the computation. Each deep meta path can be assigned to a single computation node. Furthermore, For each deep meta path, we can employ Graphics Processing Unit (*GPU*) to speed up the matrix operations for each deep meta path.

5.4 Algorithm Description.

Here, we describe the pseudo-code of the algorithm for computing $DMSS$, see algorithm 1. Step 1 aims to obtain the augmented spanning tree and its internal object types. Then, each internal object type is viewed as a pivot, and the **DeepMS** is decomposed into several deep meta paths. Step 2-14 aims to compute the commuting matrices of deep meta paths. At last, the similarity matrix $DMSS$ can be computed at step 15.

Algorithm 1 spends its most time on step 2-14. Step 3 spends $t_1 = O(N \times |\mathcal{T}_p|)$ on computing $\omega_{\mathcal{D}_p}$. Step 5-6 spend $t_{21} = |\mathcal{T}_s^2| |\mathcal{T}_c|$ on computing $\bar{W}_{\mathcal{T}_s \mathcal{T}_c}^T \bar{W}_{\mathcal{T}_s \mathcal{T}_c}$,

$t_{22} = |\mathcal{T}_c|^3$ on computing the inverse of $\mathbf{I} - \lambda \bar{W}_{\mathcal{T}_s \mathcal{T}_c}^T \bar{W}_{\mathcal{T}_s \mathcal{T}_c}$, and $t_{23} = O(|\mathcal{T}_s|^2 |\mathcal{T}_c|^2)$ on computing $\mathcal{M}_{\mathcal{D}_s}$. Overall, the total time which step 5-6 spend is $t_2 = t_{21} + t_{22} + t_{23}$. Step 11-12 spends $t_{31} = O(|\mathcal{T}_p|^2 |\mathcal{T}_c|)$ on computing $\bar{W}_{\mathcal{T}_p \mathcal{T}_c} \bar{W}_{\mathcal{T}_p \mathcal{T}_c}^T$, $t_{32} = O(|\mathcal{T}_p|^3)$ on computing the inverse of $\mathbf{I} - \lambda \bar{W}_{\mathcal{T}_p \mathcal{T}_c} \bar{W}_{\mathcal{T}_p \mathcal{T}_c}^T$, and $t_{33} = O(|\mathcal{T}_s|^2 |\mathcal{T}_p|^2 \prod_{i=1}^n |\mathcal{T}_i|^2)$ on computing $\mathcal{M}_{\mathcal{D}_p}$. Overall, the total time which step 11-12 spend is $t_3 = t_{31} + t_{32} + t_{33}$. Therefore, the time complexity of algorithm 1 is $O(|\mathcal{I}| \times (t_1 + t_2 + t_3))$. As stated previously, we can employ *GPU* and distributed computing techniques to accelerate the computations. In this paper, we can only implement it using my personal computer, because we have no GPU and distributed environments.

Algorithm 1 Computing *DMSS*

INPUT: **HIN** G , Network Schema Θ_G , Source Object Type \mathcal{T}_s Decaying Parameter $0 < \lambda < 1$.

OUTPUT: Similarity Matrix *DMSS*

- 1: Traverse Θ_G from \mathcal{T}_s , and obtain an augmented spanning tree rooted at \mathcal{T}_s . Assume \mathcal{I} denotes the set of its internal nodes.
- 2: **for** each pivotal object type $\mathcal{T}_p \in \mathcal{I}$ **do**
- 3: Compute the weight $\omega_{\mathcal{D}_p}$ of the deep meta path \mathcal{D}_p using formula 7.
- 4: **if** $\mathcal{T}_p = \mathcal{T}_s$ **then**
- 5: Construct the deep meta path \mathcal{D}_s , see the form 3.
- 6: Compute the commuting matrix $\mathcal{M}_{\mathcal{D}_s}$ of \mathcal{D}_s using formula 4.
- 7: **if** $\mathcal{M}_{\mathcal{D}_s}$ is diagonal **then**
- 8: $\mathcal{M}_{\mathcal{D}_s} \leftarrow 0$.
- 9: **end if**
- 10: **else**
- 11: Construct the deep meta path \mathcal{D}_p , see the form 5.
- 12: Compute the commuting matrix $\mathcal{M}_{\mathcal{D}_p}$ of \mathcal{D}_p using formula 6.
- 13: **end if**
- 14: **end for**
- 15: Compute *DMSS*(o_s, o_t) for any two objects o_s and o_t using formula 8.
- 16: **return** *DMSS*.

Below, we take the **HIN** shown in Fig. 1 as an example to present the procedure of computing *DMSS*. Its network schema is shown in Fig. 2. As shown in Fig. 5, its **DeepMS** can be decomposed into a deep meta path (see 5(b)) and a deep meta tree (see 5(c)). The deep meta tree can be further decomposed two deep meta paths, see Fig. 5(d,e). The commuting matrix of the deep meta path shown in Fig. 5(b) is

$$\mathcal{M}_P = \begin{bmatrix} 10.0 & 0.0 & 0.0 & 0.0 \\ 0.0 & 10.0 & 0.0 & 0.0 \\ 0.0 & 0.0 & 3.33 & 0.0 \\ 0.0 & 0.0 & 0.0 & 10.0 \end{bmatrix}.$$

This commuting matrix should be ignored because it is diagonal. The commuting matrix of the deep meta path shown in Fig. 5(d) is

$$\mathcal{M}_A = \begin{bmatrix} 2.149 & 1.247 & 1.786 & 1.247 \\ 0.623 & 2.705 & 1.714 & 1.529 \\ 0.762 & 1.476 & 2.095 & 1.476 \\ 0.623 & 1.529 & 1.714 & 2.705 \end{bmatrix}.$$

Similarly, the commuting matrix of the deep meta path shown in Fig. 5(e) is

$$\mathcal{M}_T = \begin{bmatrix} 2.978 & 0.877 & 1.666 & 1.147 \\ 1.929 & 2.305 & 1.598 & 0.971 \\ 1.885 & 0.816 & 2.020 & 1.239 \\ 1.802 & 0.694 & 1.691 & 2.433 \end{bmatrix}.$$

According to the weight-generating strategy, the weights of \mathcal{M}_A is 0.66, and that of \mathcal{M}_T is 0.34. Therefore, the similarity matrix

$$DMSS = \begin{bmatrix} 1.000 & 0.058 & 0.162 & 0.060 \\ 0.072 & 1.000 & 0.133 & 0.101 \\ 0.242 & 0.0241 & 1.000 & 0.286 \\ 0.062 & 0.098 & 0.146 & 1.000 \end{bmatrix}.$$

The rows/columns of $DMSS$ respectively represent ‘TKDE’, ‘AAAI’, ‘VLDB’ and ‘KDD’.

6 Experimental Evaluations

In this section, we compare $DMSS$ with the state-of-the-art metrics on two real datasets. As similarly as the literatures [20, 9], we also employ the ranking quality and the clustering quality to show the goodness of metrics. The configuration of my PC is Intel(R) Core(TM) i5-4570 CPU @ 3.20GHz and RAM 12GB.

6.1 Comparison Metrics

For the ranking task, we choose a popular comparison metric which is also used in papers [20, 9], called Normalized Discounted Cumulative Gain ($nDCG$) [24], to evaluate the quality of ranking. The bigger its value, the better the ranking. For the clustering task, we also choose a popular comparison metric which is used in papers [20, 9], called Normalized Mutual Information (NMI) [9], to evaluate the quality of clustering. The bigger its value, the better the clustering.

6.2 Datasets.

Three real datasets, respectively called **DBLPc**, **DBLP_r** and **BioIN**, are used here. The first two [9] are extracted from **DBLP**¹. The last is extracted from **Chem2Bio2RDF** [22, 23]. **DBLPc** includes 21 venues coming from four areas: database, data mining, information retrieval and machine learning, 25858 papers, 25780 authors and 10436 terms. **DBLP_r** includes 20 venues, 23906 papers, 24078 authors and 9862 terms. Their network schema is shown in Fig. 2(a). **BioIN** includes 2018 genes, 300 tissues, 4331 gene ontology instances, 224 substructures, 712 side effects and 18097 chemical compounds. Its network schema is shown in Fig. 2(b). Note in particular that we only consider the genes assigned to a single cluster here because we use k-means algorithm to cluster the genes. The **DeepMS** for **DBLPc** is shown in Fig. 5(a), and for **BioIN** is shown in Fig. 6(a).

6.3 Baselines.

In this paper, *DMSS* is compared with three state-of-the-art similarity metrics: *BSCSE* [20], *BPCRW* [15, 14], *PathSim* [9]. Let \mathcal{P} and \mathcal{S} respectively denote a meta path and a meta structure. For a given source-target object pair (o_s, o_t) , they are defined as follows.

$$BSCSE(g, i | \mathcal{S}, o_t) = \frac{\sum_{g' \in \sigma(g, i | \mathcal{S}, G)} BSCSE(g', i + 1 | \mathcal{S}, o_t)}{|\sigma(g, i | \mathcal{S}, G)|^\alpha}.$$

$$BPCRW(o, o_t | \mathcal{P}) = \frac{\sum_{o' \in N_{\mathcal{P}}(o)} BPCRW(o', o_t | \mathcal{P})}{|N_{\mathcal{P}}(o)|^\alpha}.$$

$$PathSim(o_s, o_t | \mathcal{P}) = \frac{2 \times \mathcal{M}_{\mathcal{P}}(o_s, o_t)}{\mathcal{M}_{\mathcal{P}}(o_s, o_s) + \mathcal{M}_{\mathcal{P}}(o_t, o_t)}.$$

In these definitions, α is a biased parameter. For *BSCSE*, $\sigma(g, i | \mathcal{S}, G)$ denotes the $(i + 1)$ -th layer's instances expanded from $g \in \mathcal{S}[1 : i]$ on G [20]. For *BPCRW*, $N_{\mathcal{P}}(o)$ denotes the neighbors of o along meta path \mathcal{P} [15, 14]. For *PathSim*, $\mathcal{M}_{\mathcal{P}}$ denotes the commuting matrix of the meta path \mathcal{P} [9].

6.4 Parameter Setting.

BSCSE and *BPCRW* involve an input parameter α . In this paper, α is set to 0.1, 0.3, 0.5, 0.7 and 0.9. Then, we respectively select the maximum *NMI* (clustering quality) and the maximum *nDCG* (ranking quality) under these parameter settings. For the proposed metric *DMSS*, its decaying parameter λ is set to 0.1, 0.2, 0.3, 0.4, 0.5, 0.6, 0.7, 0.8, 0.9. Below, we compare the *NMI* and *nDCG* under these parameter settings with those yielded by *PathSim*, *BPACRW* and *BSCSE*.

¹ <http://dblp.uni-trier.de/db/>

6.5 Clustering Quality.

Now, we compare *DMSS* with the baselines in terms of clustering quality (*NMI* [9], the bigger, the better) on **DBLPc** and **BioIN**. First, we compute the similarities between two objects respectively using these metrics. That means we obtain a feature vector for each object. Then, we employ *k*-means algorithm to cluster these feature vectors (i.e. the objects). For **DBLPc**, *Venue* is selected as the source and target object type. Its benchmark is given according to the scope of the venues. For **BioIN**, *Gene* is set to the source and target object type. Its benchmark is extracted from the one used in paper [26]. *k* is set to the number of clusters in the benchmark. In section 6.5.1, we illustrate the sensitivity of the state-of-the-art metrics to different schematic structures in terms of *NMI*. In sections 6.5.2 and 6.5.3, we respectively compare the proposed method *DMSS* with the state-of-the-art metrics in terms of *NMI* on **DBLPc** and **BioIN**.

6.5.1 Sensitivity in terms of *NMI*.

As stated previously, the proposed *DMSS* is robust (insensitive) to schematic structures, because it combines all the possible schematic structures in the form of deep meta paths. Here, we aim to evaluate the sensitivity of the state-of-the-art metrics (*PathSim*, *BPCRW* and *BSCSE*) in terms of clustering task, because all of them takes a kind of schematic structure (meta path or meta structure) as input.

On **DBLPc**, two kinds of meta paths, i.e. (V, P, A, P, V) and (V, P, T, P, V) , are selected for *PathSim* and *BPCRW*, and we then compare the *NMI* values under these two meta paths and different biased parameters α . On **BioIN**, four kinds of meta paths, i.e. (G, GO, G) , (G, T, G) , (G, CC, Si, CC, G) and (G, CC, Sub, CC, G) , are selected for *PathSim* and *BPCRW*. Two kinds of meta structures, i.e. $(G, (GO, T), G)$ and $(G, CC, (Si, Sub), CC, G)$, are selected for *BSCSE*. Then, we compare the *NMI* values under these schematic structures and different biased parameters α . Note in particular *PathSim* does not depend on any parameters. Therefore, its lines with different meta paths is parallel to x-axis.

Fig. 9 and Fig. 10 respectively show the *NMI* values under different α for *BPCRW*, *PathSim* with different meta paths on **BioIN**. Fig. 11 shows the *NMI* values under different α for *BSCSE* with different meta structures on **BioIN**. For *PathSim* and *BPCRW*, the *NMI* values with (G, GO, G) are much larger than those with the other meta paths. For *BSCSE*, the *NMI* values with $(G, (GO, T), G)$ are much larger than that with $(G, CC, (Si, Sub), CC, G)$. This reveals *PathSim* and *BPCRW* are sensitive to meta paths, and *BSCSE* is sensitive to meta structures.

Fig. 12 and 13 respectively show the *NMI* values under different α for *PathSim* and *BPCRW* with different meta paths on **DBLPc**. Note in particular that we do not consider the sensitivity of *BSCSE* to different meta structures because the meta structure $(V, P, (A, T), P, V)$ is most frequently used

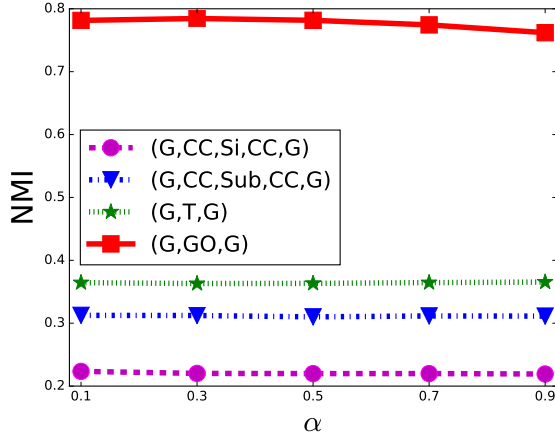


Fig. 9 Sensitivity of *BPCRW* to different schematic structures on **BioIN** in terms of clustering.

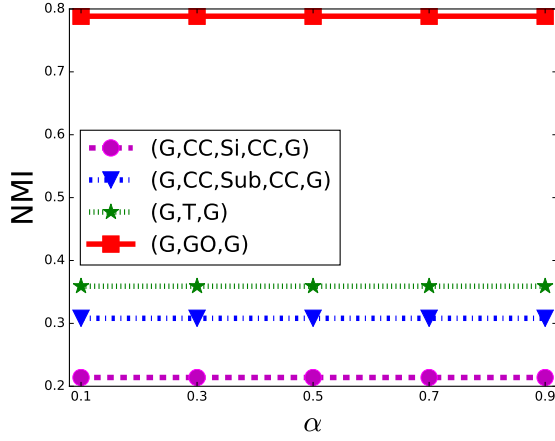


Fig. 10 Sensitivity of *PathSim* to different schematic structures on **BioIN** in terms of clustering.

on DBLP_r. According to these figures, we know that *BPCRW* and *PathSim* are also sensitive to different meta paths on DBLP_r.

To be summarized, all of the baselines are sensitive to different schematic structures on **BioIN** and **DBLP_c**. This suggests that it is important for the baselines to select an appropriate schematic structures. The proposed metric *DMSS* does not depend on any schematic structures. This is the biggest advantage of *DMSS* relative to the baselines.

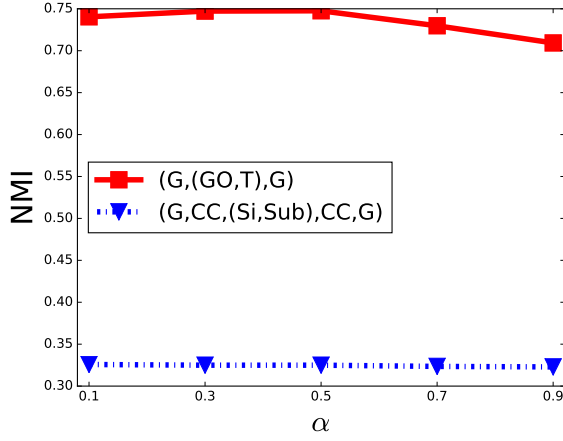


Fig. 11 Sensitivity of *BSCSE* to different schematic structures on **BioIN** in terms of clustering.

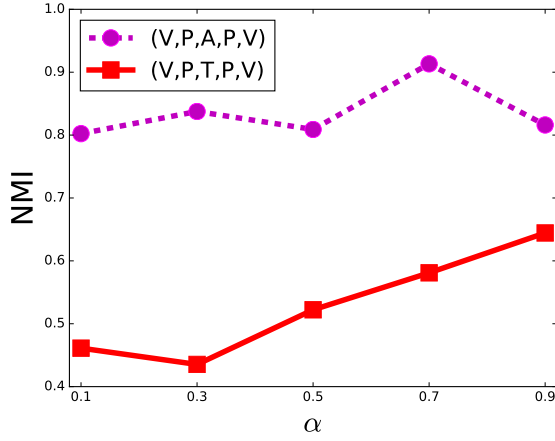


Fig. 12 Sensitivity of *BPCRW* to different meta paths **DBLPc** in terms of clustering.

6.5.2 On BioIN.

Here, we compare the *NMI* values yielded by *DMSS* with those yielded by the baselines under different decaying parameters λ on **BioIN**. Note in particular that for *BSCSE* and *BPCRW*, their *NMI* values are the optimal ones under different biased parameters α .

As shown in Fig. 14, the optimal *NMI* yielded by *PathSim* is larger than that yielded by *BSCSE* and *BPCRW*. When $\lambda = 0.7, 0.8, 0.9$, the *NMI* values yielded by *DMSS* is larger than that yielded by *PathSim*. When $\lambda = 0.1, 0.2, \dots, 0.6$, the *NMI* values yielded by *DMSS* is less than those

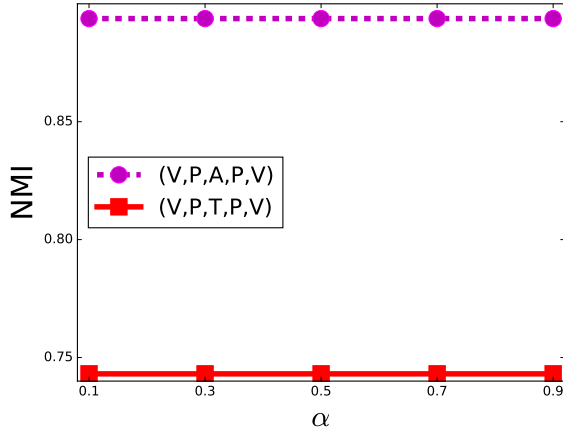


Fig. 13 Sensitivity of *PathSim* to different meta paths on **DBLPc** in terms of clustering.

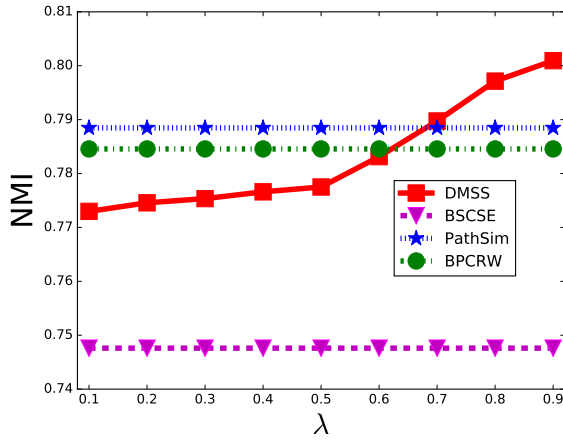


Fig. 14 Comparison of *NMI* for *DMSS* under different λ with optimal *NMI* for *PathSim*, *BSCSE* and *BPCRW* on **BioIN**.

yielded by *PathSim* and *BPCRW*. In addition, we discover that the difference between the *NMI* values yielded by *DMSS* and the ones yielded by *PathSim* is less than 0.02 according to this figure. Overall, *DMSS* is comparable to *PathSim* and *BPCRW* on the whole, but outperforms *BSCSE*.

6.5.3 On DBLPc.

Here, we compare the *NMI* values yielded by *DMSS* with those yielded by the baselines under different decaying parameters λ on **DBLPc**. Note in

particular that for *BSCSE* and *BPCRW*, their *NMI* values are the optimal ones under different biased parameters α .

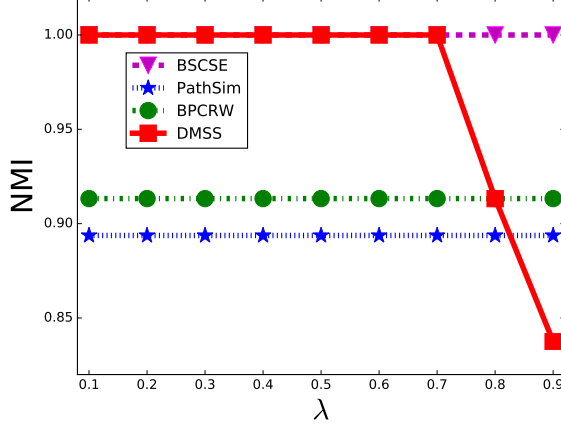


Fig. 15 Comparison of *NMI* for *DMSS* under different λ with optimal *NMI* for *PathSim*, *BSCSE* and *BPCRW* on **DBLPc** in terms of clustering.

As shown in Fig. 15, the optimal *NMI* yielded by *BSCSE* is larger than that yielded by *BSCSE* and *BPCRW*. When $\lambda = 0.1, 0.2, \dots, 0.7$, the *NMI* values yielded by *DMSS* reach the maximum 1.0. At this time, this value is equal to those yielded by *BSCSE*. When $\lambda = 0.8$, the *NMI* value yielded by *DMSS* is less than that yielded by *BSCSE* but no less than *BPCRW* and *PathSim*. When $\lambda = 0.9$, the *NMI* value yielded by *DMSS* reaches its minimum 0.837541. At this time, this value is less than the optimal values yielded by the baselines. According to our experimental results, we know that (1) the maximum *NMI* value yielded by *BSCSE* is equal to 1.0 only when its biased parameter α takes 0.9; (2) the minimum *NMI* value yielded by *BSCSE* is equal to 0.793139. That means that (1) the *NMI* values yielded by *DMSS* reach its maximum at more parameter settings; (2) the minimum *NMI* value yielded by *DMSS* is larger than that yielded by *BSCSE*.

6.6 Ranking Quality.

Now, we compare *DMSS* with the baselines in terms of ranking quality (*nDCG* [9], the higher, the better) on **DBLP**. First, we select three venues ‘KDD’, ‘TKDE’ and ‘SIGMOD’ as our source objects. For each source object, all the venues can be ranked as 0 (unrelated), 1 (slightly related), 2 (fairly related), 3 (highly related) according to the similarities between the source object and them. Then, we employ *DMSS* and the other baselines to compute the similarities between the source objects and the other venues. As a

result, we obtain $nDCG$ values respectively for the source objects. In section 6.6.1, we illustrate the sensitivity of the state-of-the-art metrics to different schematic structures in terms of $nDCG$. In section 6.6.2, we compare the proposed *DMSS* with the state-of-the-art metrics in terms of $nDCG$ on **DBLPc**.

6.6.1 Sensitivity in terms of $nDCG$.

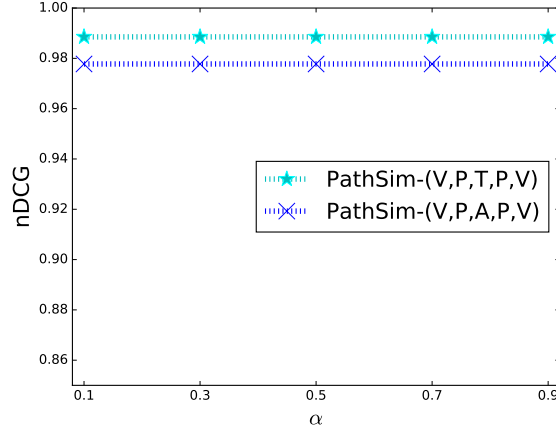


Fig. 16 Sensitivity of *PathSim* to different meta paths on **DBLPc** in terms of ranking with KDD as the source object.

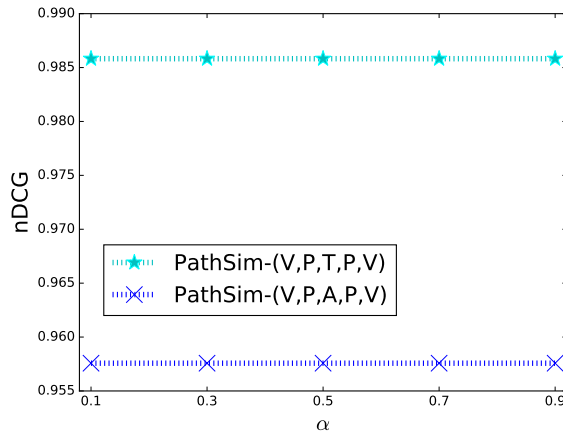


Fig. 17 Sensitivity of *PathSim* to different meta paths on **DBLPc** in terms of ranking with SIGMOD as the source object.

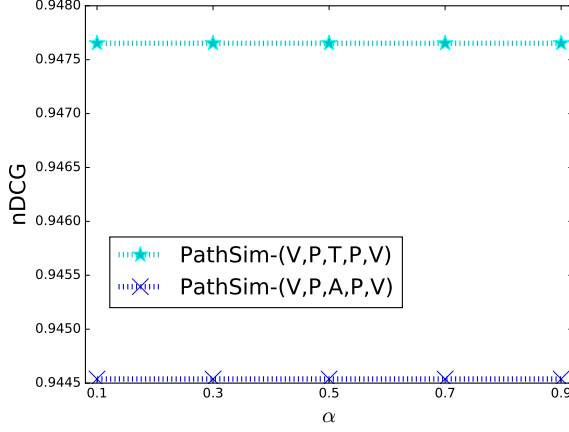


Fig. 18 Sensitivity of *PathSim* to different meta paths on **DBLP** in terms of ranking with TKDE as the source object.

Here, we investigate whether *PathSim* and *BPCRW* are sensitive to different meta paths in terms of ranking task as similarly as the section 6.5.1. Fig. 16, Fig. 17 and Fig. 18 respectively shows the *nDCG* values of *PathSim* under different meta paths when respectively selecting KDD, SIGMOD and TKDE as the source objects. Fig. 19, Fig. 20 and Fig. 21 respectively shows the *nDCG* values of *BPCRW* under different meta paths when respectively selecting KDD, SIGMOD and TKDE as the source objects. According to these figures, we know that the *nDCG* values for the meta path (V, P, A, P, V) is always larger than that for the meta path (V, P, T, P, V) . This means *PathSim* and *BPCRW* are sensitive to different meta paths in terms of ranking task.

6.6.2 Ranking Quality.

Now, we compare the *nDCG* values yielded by *DMSS* and the baselines when selecting three source venues KDD, SIGMOD and TKDE. For *BPCRW* and *BSCSE*, their maximum *nDCG* values under different biased parameters α are considered here. For *DMSS*, its decaying parameter is respectively set to 0.1, 0.2, \dots , 0.9.

Fig. 22(a) shows the *nDCG* values under different decaying parameters λ when selecting KDD as the source venue. This figure reveals that (1) the *nDCG* values yielded by *PathSim* is larger than those yielded by *BPCRW* and *BSCSE*; (2) the *nDCG* values yielded by *DMSS* is larger than those yielded by *PathSim* when λ takes 0.6, 0.7, 0.8, 0.9; (3) the *nDCG* values yielded by *DMSS* is less than those yielded by *PathSim* when λ takes 0.1, 0.2, 0.3, 0.4, 0.5, but larger than those yielded by *BPCRW* and *BSCSE*.

Fig. 23 and Fig. 24 shows the *nDCG* values under different decaying parameters λ when respectively selecting SIGMOD and TKDE as the source

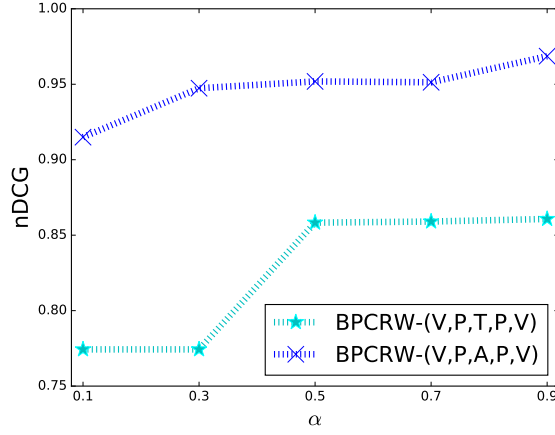


Fig. 19 Sensitivity of *BPCRW* to different meta paths on **DBLP** in terms of ranking with KDD as the source object.

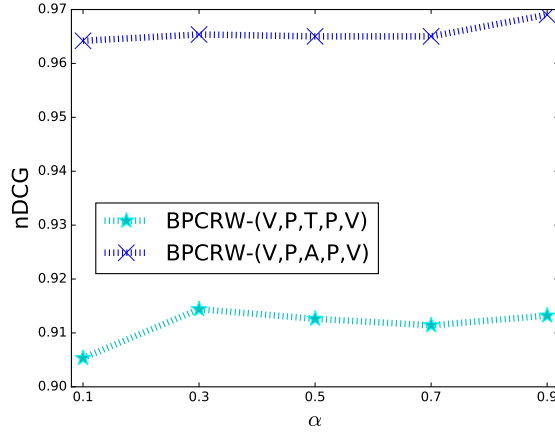


Fig. 20 Sensitivity of *BPCRW* to different meta paths on **DBLP** in terms of ranking with SIGMOD as the source object.

venue. This figure reveals that the $nDCG$ values yielded by *DMSS* is always larger than those yielded by the baselines no matter what λ takes.

In summary, *DMSS* on the whole performs better than the baselines in terms of the ranking task.

6.7 Time Efficiency.

Here, we evaluate the time efficiency of *DMSS*, *BPCRW*, *PathSim* and *BSCSE* on **BioIN**, **DBLPc** and **DBLP**. Table 1 shows the running time of

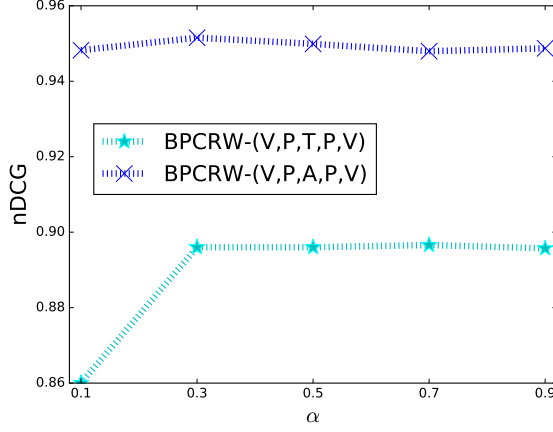


Fig. 21 Sensitivity of *BPCRW* to different meta paths on **DBLP** in terms of ranking with TKDE as the source object.

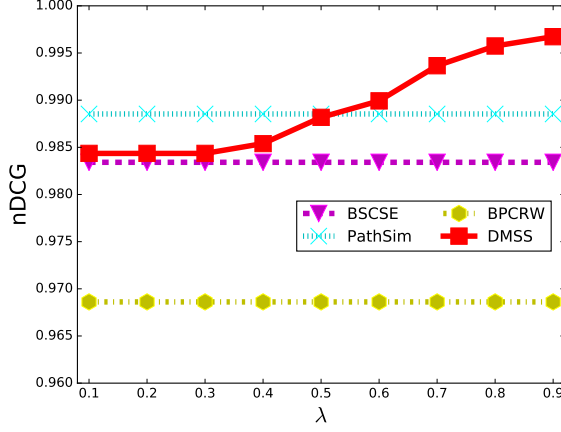


Fig. 22 The comparison of *nDCG* values under different the decaying parameters λ . KDD is the source object.

computing the similarities between any two objects using these metrics. According to this table, we know that *BPCRW* performs better than the other metrics in terms of time efficiency. *DMSS* has no significant advantages in terms of time efficiency. This is consistent with our expectation, because computing *DMSS* requires a lot of matrix multiplication operations. As stated in section 5.3, the distributed computing techniques can be easily employed here. Specifically, the commuting matrix for each deep meta path is assigned to a single computation node. In addition, we can also employ *GPU* to speed up the matrix multiplications. This means the time efficiency can be improved

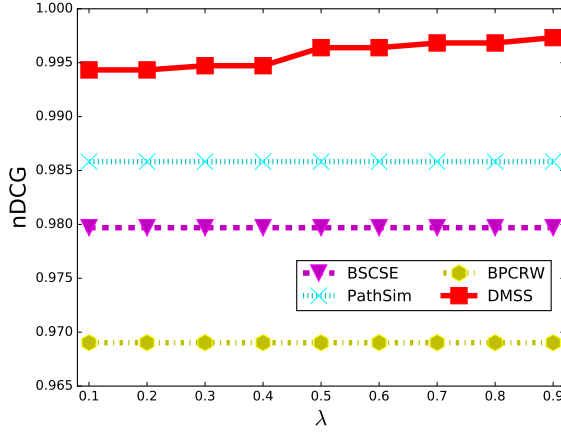


Fig. 23 The comparison of $nDCG$ values under different the decaying parameters λ . SIG-MOD is the source object.

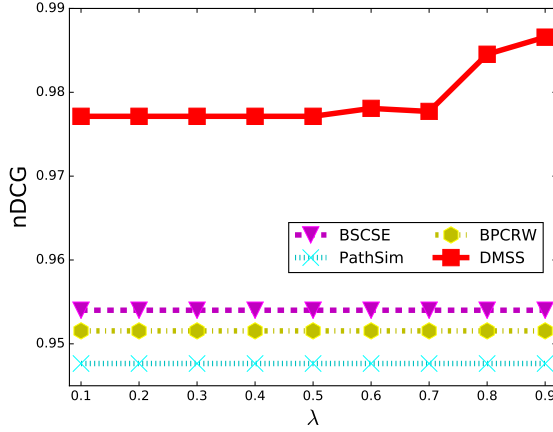


Fig. 24 The comparison of $nDCG$ values under different the decaying parameters λ . TKDE is the source object.

significantly. Unfortunately, we have no **GPU** and the distributed computing environment. It is noteworthy that the proposed *DMSS* is insensitive to different meta paths and meta structures and outperforms the state-of-the-art metrics in terms of clustering and ranking task. This is the biggest advantage.

Furthermore, we discover that the running time of *BSCSE* on **DBLPc** and **DBLP** is much larger than that on **BioIN**. This is because the nature of **DBLPc** and **DBLP** is different from that of **BioIN**. On **DBLPc** or **DBLP**, we only consider the meta structure $(V, P, (A, T), P, A)$. Each venue contains a lot of papers. This causes too many author-paper pairs. The algo-

Table 1 Average Running Time (Sec) of computing similarity between a source and a target object.

Metric \ DataSet	DBLPc	DBLPi	BioIN
<i>BPCRW</i>	10.407	9.709	5.320
<i>PathSim</i>	229.642	162.693	630.083
<i>BSCSE</i>	10305.906	9896.015	9.913
<i>DMSS</i>	8159.485	6645.529	555.786

rithm for computing *BSCSE* spends too much time on traversing these pairs. On **BioIN**, we consider two meta structures $(G, CC, (Si, Sub), CC, G)$ and $(G, (GO, Ti), G)$. For $(G, (GO, Ti), G)$, each gene links to a small number of pairs whose entries respectively belong to *GO* and *Ti*. For $(G, CC, (Si, Sub), CC, G)$, each gene links to a small number of chemical compounds and these chemical compounds link to a small number of pairs whose entries respectively belong to *Si* and *Sub*. Therefore, The algorithm for computing *BSCSE* spends a little time on traversing these pairs.

7 Conclusion

In this paper, we propose *DMSS*, a deep meta structure based similarity metric on **HINs**. It can be constructed automatically. To extract semantics encapsulated in the **DeepMS**, we first decompose it into several deep meta paths, and then combine the commuting matrices of the deep meta paths according to different weights. As a result, *DMSS* is defined by the combination of these commuting matrices. Experimental evaluations show that (1) *PathSim*, *BPCRW* and *BSCSE* are sensitive to meta paths or meta structures; (2) *DMSS* on the whole outperforms the baselines in terms of clustering and ranking. In future, a promising direction is to employ parallel computing techniques to accelerate the computation of *DMSS*.

References

1. Y. Sun and J. Han and P. Zhao and Z. Yin and H. Cheng and T. Wu, *RankClus: Integrating Clustering with Ranking for Heterogeneous Information Network Analysis*, In Proceedings of the 12-th International Conference on Extending Database Technology, pp. 565-576, 2009.
2. Y. Sun and Y. Yu and J. Han, *Ranking-based clustering of heterogeneous information networks with star network schema*, In Proceedings of the ACM SIGKDD International Conference on Knowledge Discovery and Data Mining, pp. 797-806, 2009.
3. Y. Sun and J. Han, *Mining heterogeneous information networks: a structural analysis approach*, SIGKDD Explorations, 14 (2012), pp. 20-28.
4. C. Shi and Y. Li and J. Zhang and Y. Sun and P.S. Yu, *A Survey of Heterogeneous Information Network Analysis*, IEEE Transactions on Knowledge and Data Engineering, 29 (2017), pp. 17-37.
5. J. Han, M. Kamber and J. Pei, *Data Mining: Concepts and Techniques (3rd)*, Morgan Kaufmann, Waltham, 2012.

6. G. Jeh and J. Widom, *SimRank: a measure of structural-context similarity*, In Proceedings of the 8-th ACM SIGKDD International Conference on Knowledge Discovery and Data Mining, pp. 538-543, 2002.
7. G. Jeh and J. Widom, *Scaling Personalized Web Search*, In Proceedings of the 12-th International Conference on World Wide Web, pp. 271-279, 2003.
8. V. Martinez and F. Berzal and J.C. Cubero. *A survey of link prediction in complex networks*, ACM Computing Surveys, 49 (4), pp. 69:1-69:33.
9. Y. Sun and J. Han and X. Yan and P.S. Yu and T. Wu, *PathSim: Meta Path-based top-k similarity search in heterogeneous information networks*, In Proceedings of the VLDB Endowment, pp. 992-1003, 2011.
10. B. Usman and I. Oseledets. *Tensor SimRank for Heterogeneous Information Networks*, In Proceedings of the ACM SIGKDD International Conference on Knowledge Discovery and Data Mining, pp. 89-97, 2015.
11. C. Wang and Yizhou Sun and Y. Song and J. Han et al. *RelSim: Relation Similarity Search in Schema-Rich Heterogeneous Information Networks*, In Proceedings of the Siam International Conference on Data Mining, pp. 621-629, 2016
12. Y. Xiong and Y. Zhu and P.S. Yu, *Top-k similarity join in heterogeneous information networks*, IEEE Transactions on Knowledge and Data Engineering, 27 (2015), pp. 1710-1723.
13. C. Shi and X. Kong and Y. Huang and P.S. Yu and B. Wu, *HeteSim: A General Framework for Relevance Measure in Heterogeneous Networks*, IEEE Transactions on Knowledge and Data Engineering, 26 (2014), pp. 2479-2492.
14. N. Lao and W.W. Cohe, *Relational retrieval using a combination of path-constrained random walks*, Machine Learning, 81 (2010), pp. 53-67.
15. N. Lao and W.W. Cohen, *Fast query execution for retrieval models based on path-constrained random walks*, In Proceedings of the ACM SIGKDD International Conference on Knowledge Discovery and Data Mining, pp. 881-888, 2010.
16. Y. Sun and B. Norick and J. Han and X. Yan and P.S. Yu and X. Yu, *Integrating meta-path selection with user-guided object clustering in heterogeneous information networks*, In Proceedings of the ACM SIGKDD International Conference on Knowledge and Data Mining, pp. 1348-1356, 2012.
17. C. Shi and R. Wang and Y. Li and P.S. Yu and B. Wu, *Ranking-based Clustering on General Heterogeneous Information Networks by Network Projection*, In Proceedings of the ACM CIKM International Conference on Information and Knowledge Management, pp. 699-708, 2014.
18. Y. Sun and C.C. Aggarwal and Jiawei Han, *Relation strength-aware clustering of heterogeneous information networks with incomplete attributes*, Proceedings of the VLDB Endowment, 5 (2012), pp. 394-405.
19. B. Chen and Y. Ding and D.J. Wild, *Assessing Drug Target Association Using Semantic Linked Data*, PLoS Computational Biology, 8 (2012), pp. 1-10.
20. Z. Huang and Y. Zheng and R. Cheng and Y. Zhou and N. Mamoulis and X. Li, *Meta Structure: Computing Relevance in Large Heterogeneous Information Networks*, In Proceedings of the ACM SIGKDD International Conference on Knowledge Discovery and Data Mining, pp. 1595-1604, 2016.
21. T. Sauer, *Numerical Analysis (2nd)*, Addison-Wesley, New Jersey, 2012.
22. B. Chen and X. Dong and D. Jiao and H. Wang and Q. Zhu and Y. Ding and D.J. Wild, *Chem2Bio2RDF: a semantic framework for linking and data mining chemogenomic and systems chemical biology data*, BMC Bioinformatics, 11 (2010), pp. 3011-3015.
23. G. Fu and Y. Ding and A. Seal and B. Chen and Y. Sun and E. Bolton, *Predicting drug target interactions using meta-path-based semantic network analysis*, BMC Bioinformatics, 17 (2016), pp. 1-10.
24. Y. Wang and L. Wang and Y. Li and D. He and W. Chen and T.Y. Liu, *A Theoretical Analysis of Normalized Discounted Cumulative Gain (NDCG) Ranking Measures*, In Proceedings of the 26-th Annual Conference on Learning Theory, pp. 1-30, 2013.
25. D. M. W. Powers, *Evaluation: From Precision, Recall and F-Measure to ROC, Informedness, Markedness and Correlation*, Journal of Machine Learning Technology, 2 (2011), pp. 37-63.

26. S. Jia and L. Gao and Y. Gao and J. Nastos and Y. Wang and X. Zhang and H. Wang, *Defining and identifying cograph communities in complex networks*, New Journal of Physics, 17 (2015), pp. 013044.
27. Bach and Francis R., *Graph Kernels Between Point Clouds*, In Proceedings of the 25th International Conference on Machine Learning, pp. 25-32, 2008.
28. N. Shervashidze and P. Schweitzer and E.J. van Leeuwen and K. Mehlhorn and K.M. Borgwardt, *Weisfeiler-Lehman Graph Kernels*, Journal of Machine Learning Research, 12 (2011), pp. 2539–2561.
29. Y. Yang and J. Tang and C. Leung and Y. Sun and Q. Chen and J. Li and Q. Yang, *RAIN: Social Role-Aware Information Diffusion*, In Proceedings of the 29th AAAI Conference on Artificial Intelligence, pp. 367-373, 2015.
30. C. Wang and J. Han and Y. Jia and J. Tang and D. Zhang and Y. Yu and J. Guo, *Mining advisor-advisee relationships from research publication networks*, In Proceedings of the 16th ACM SIGKDD International Conference on Knowledge Discovery and Data Mining, pp. 203-212, 2010.
31. F. Zhu and Q. Qiang and D. Lo and X. Yan and J. Han and P.S. Yu, *Mining Top-K Large Structural Patterns in a Massive Network*, Proceedings of VLDB Endowment, 4 (2011), pp. 807-818.